Model formulation and determination of in vitro parameters of a noninvasive method to calculate flexor tendon forces in the equine forelimb

Liduin S. Meershoek, PhD; Anton J. van den Bogert, PhD; Henk C. Schamhardt, PhD†

Objective—To describe a method to calculate flexor tendon forces on the basis of inverse dynamic analysis and an in vitro model of the equine forelimb and to quantify parameters for the model.

Sample Population—38 forelimbs of 23 horses that each had an estimated body mass of ≥ 500 kg.

Procedure—Longitudinal limb sections were used to determine the lines of action of the tendons. Additionally, limb and tendon loading experiments were performed to determine mechanical properties of the flexor tendons.

Results—The study quantified the parameters for a pulley model to describe the lines of action. Furthermore, relationships between force and strain of the flexor tendons and between fetlock joint angle and suspensory ligament strain were determined, and the ultimate strength of the tendons was measured.

Conclusion and Clinical Relevance—The model enables noninvasive determination of forces in the suspensory ligament, superficial digital flexor tendon, and distal part of the deep digital flexor (DDF) tendon. In addition, it provides a noninvasive measure of loading of the accessory ligament of the DDF tendon for within-subject comparisons. However, before application, the method should be validated. The model could become an important tool for use in research of the cause, prevention, and treatment of tendon injuries in horses. (*Am J Vet Res* 2001;62:1585–1593)

Athletic horses often have overload-induced injuries in the forelimb flexor tendons. Quantification of tendon loads can provide useful information for investigations of the causes, prevention, and treatment of those injuries. Tendon loads can be measured invasively, using implanted force or strain transducers[1-3]; however, this is limited by ethical and practical problems. Some tendon loads can be determined noninvasively. Bartel et al[4] described a method based on inverse dynamic analysis to determine the force on the **deep digital flexor (DDF)** tendon and a measure of the combined forces of the **superficial digital flexor (SDF)** tendon and **suspensory ligament (SL)**. Jansen et al[5] described a method to determine strain in the SL on the basis of angles of the **metacarpophalangeal joint (fetlock joint)**. However, neither method enables the determination of all tendon forces and strains, including those of the SDF tendon, a tendon that is often injured.[6]

Inverse dynamic analysis typically results in estimates of net joint moments. These moments represent the total influence of all tendons acting across the joint. Most often, the number of tendons exceeds the number of joints, and there are an infinite number of combinations of tendon forces that result in the same net joint moments. This problem is the classic indeterminacy problem that typically is solved by assuming that some muscles are inactive, using **electromyography (EMG)** data or a mathematic optimization.[7-9] However, validation of these methods has produced mixed results.[10,11] Furthermore, there are many predominantly tendinous structures in the equine forelimb. It is unlikely that load distribution between active and passive structures can be described adequately with optimization criteria. Moreover, forces in the passive structures are not represented in electromyographic information. Therefore, EMG or mathematic optimization does not appear to be a useful option to quantify tendon loading in the equine forelimb.

Loading of passive structures depends on their momentary length, which can be estimated from kinematic data. The existence of such structures in the equine forelimb provides additional information that can be used to solve the indeterminacy problem. The study reported here describes a method to calculate flexor tendon forces during the stance phase. Calculations are based on an in vitro model of the equine forelimb. The objective of the study was to quantify parameters for the model. A preliminary description of the method has been published elsewhere.[12]

Materials and Methods

Proposed method for force calculation—The method combines inverse dynamic analysis[13,14] with a model of the equine forelimb. Standard inverse dynamic analysis uses

Received Oct 5, 2000.
Accepted Jan 12, 2001.
From the Department of Veterinary Anatomy and Physiology and Institute for Fundamental and Clinical Human Movement Sciences, Faculty of Veterinary Medicine, Utrecht University, Utrecht, The Netherlands (Meershoek, Schamhardt); and the Department of Biomedical Engineering, Cleveland Clinic Foundation, 9500 Euclid Ave (Wb-3), Cleveland, OH 44195 (van den Bogert). Dr. Meershoek's present address is Biomechanics and Locomotor Pathology of the Horse, Ecole Nationale Vétérinaire d'Alfort, 7 Avenue du Général de Gaulle, 94700 Maisons-Alfort, France.
Supported by grant R 87-287 of the Netherlands Organization for Scientific Research (NWO).
The authors thank Wim Kersten, Onno van der Veen, and Dr. Maarten Bobbert for technical assistance.
†Deceased.

measured ground-reaction forces and kinematics to calculate net joint moments. These net moments are equal to the product of force times moment arm summed for the tendons. The moment arms can be determined from kinematics, using a pulley model of the tendon line of action.[a] However, the major concern is to solve the indeterminacy problem. We determined a solution of this problem for the distal interphalangeal (coffin) and fetlock joints. This solution enables calculation of flexor tendon forces on the basis of net joint moments, joint angles, and moment arms.

The DDF tendon is the only tendon that can generate a flexor coffin joint moment. **Force in the distal part of the DDF tendon ($F_{DDF,dist}$)** can be calculated from the **coffin joint moment (M_{coffin})** with the assumption that there are not any extensor forces, using the following equation:

$$F_{DDF,dist} = \frac{M_{coffin}}{d_{DDF,coffin}}$$

where $d_{DDF,coffin}$ is the moment arm of the DDF tendon at the coffin joint. The $F_{DDF,dist}$ originates partly from the **accessory ligament of the DDF tendon (AL)** and partly from the muscle belly. Forces in the AL and muscle belly can be separated, using the fact that the AL and distal part of the tendon form a tendinous bone-to-bone connection. The **momentary length of AL and distal part of the DDF tendon ($L_{AL+DIST}$)** is linearly related to the **strain in the AL (ε_{AL})** and the **strain in the distal part of the DDF tendon (ε_{DIST})**, as described by the following equation:

$$L_{AL+DIST} = (c_1 \times \varepsilon_{AL}) + (c_2 \times \varepsilon_{DIST}) + c_3$$

where c_1, c_2, and c_3 are constants that are determined from in vitro experiments. The ε_{AL} can be calculated if ε_{DIST} is calculated from $F_{DDF,dist}$, using the strain-force relationship, and $L_{AL+DIST}$ is calculated from kinematics, using a pulley model. Subsequently, **force in the AL (F_{AL})** is obtained from ε_{AL}, using the strain-force relationship. **Force in the proximal part of the DDF tendon ($F_{DDF,prox}$)** then is calculated by subtracting F_{AL} from $F_{DDF,dist}$.

The SL forms an almost completely tendinous bone-to-bone connection that spans only the fetlock joint. The momentary force depends only on the momentary length, which depends only on the angle of the fetlock joint. **Force in the SL (F_{SL})** is calculated from the angle of the fetlock joint, using the joint angle-strain and strain-force relationships determined in vitro.

After the preceding steps, **force in the SDF tendon (F_{SDF})** is the only remaining unknown flexor tendon force. This force is calculated from the difference between the **fetlock joint moment calculated from inverse dynamics ($M_{fetlock}$)** and the moments generated by the SL and DDF ten-

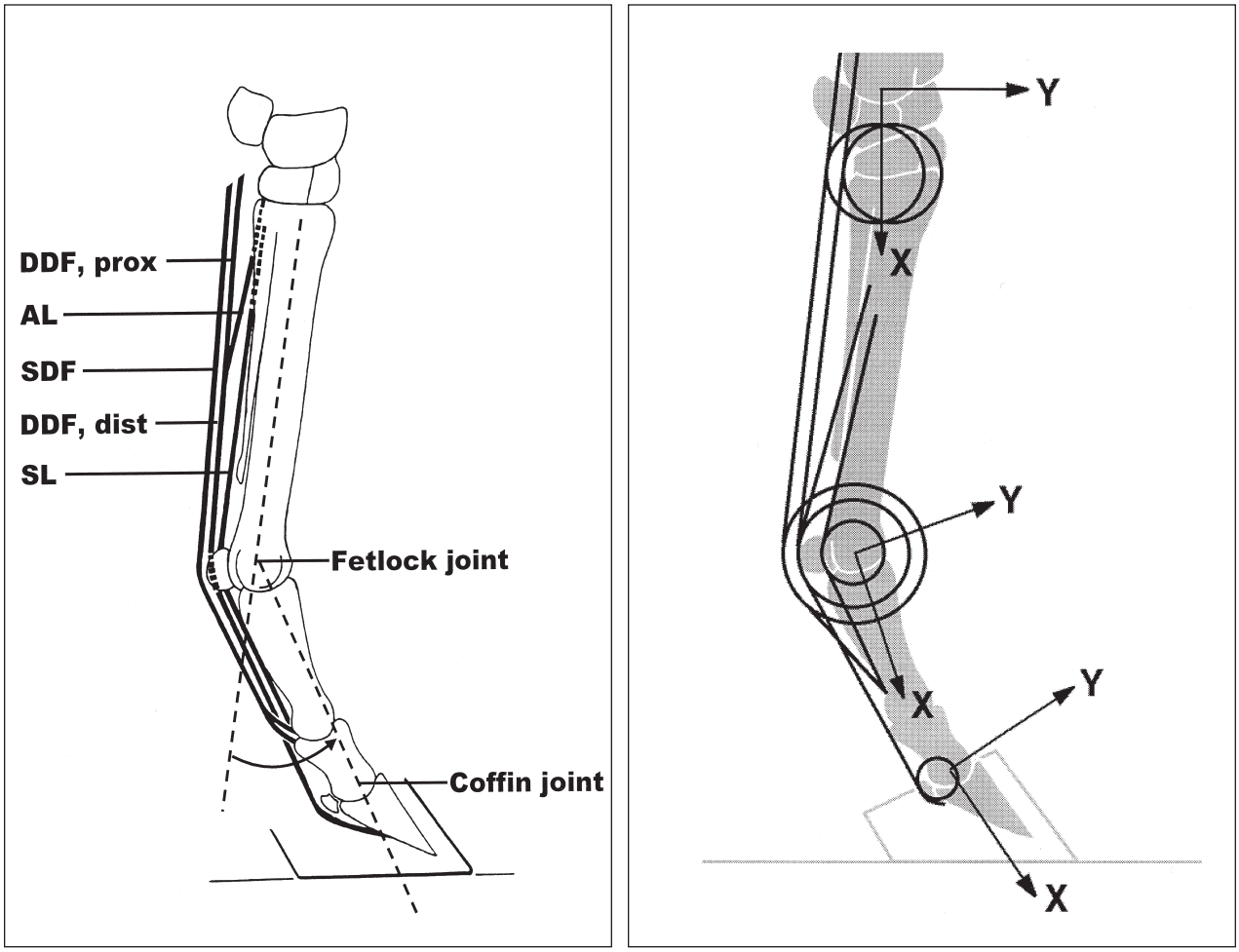

Figure 1—Anatomic depiction of the equine forelimb with angle of the metacarpophalangeal joint (fetlock joint) indicated (curved arrow; left) and pulley models of the lines of action of the tendons with definition of the segment-based coordinate systems (right). AL = Accessory ligament of the deep digital flexor (DDF) tendon. DDF,prox = Proximal part of the DDF tendon. DDF,dist = Distal part of the DDF tendon. SDF = Superficial digital flexor (SDF) tendon. SL = Suspensory ligament. Coffin joint = Distal interphalangeal joint.

don, again with the assumption that there are not any extensor forces, by use of the following equation:

$$F_{SDF} = \frac{M_{fetlock} - (F_{DDFdist} \times d_{DDFfetlock}) - (F_{SL} \times d_{SL})}{d_{SDF}}$$

where $d_{DDFfetlock}$, d_{SDF}, and d_{SL} are the moment arms of the DDF and SDF tendons and SL at the fetlock joint. Strain in the SDF tendon is determined from F_{SDF}, using the strain-force relationship determined in vitro.

To enable us to perform these calculations, parameters for several models and relationships must be quantified in vitro. These are the pulley models, to calculate $L_{AL+DIST}$ and moment arms of SL, the SDF tendon, and the DDF tendon; strain-force relationships of the SDF tendon, SL, distal and proximal parts of the DDF tendon, and AL; relationship between angle of the fetlock joint and ε_{SL}; and the relationship between $L_{AL+DIST}$, ε_{DIST}, and ε_{AL}. Additional determination of ultimate strength of the tendons enables comparison of actual loads with loads that cause failure.

Sample population—The forelimbs (18 left and 20 right) of 23 horses with an estimated body mass of ≥ 500 kg were obtained from necropsy specimens. Forelimbs were disarticulated at the shoulder joint and stored frozen until the experiments. Forelimbs for the tendon loading experiments were thawed overnight. During these experiments, the tendons were kept wet with saline (0.9% NaCl) solution.

Pulley models—Lines of action of the tendons are described by the origin, insertion, and 1 or more pulleys.[a] For the SL, 1 pulley centered at the fetlock joint was used (**Fig 1**). For the DDF tendon, 3 pulleys were used (1 attached to the hoof segment, 1 centered around the fetlock joint, and 1 attached to the metacarpal segment at the level of the carpal joint). For the SDF tendon, 2 pulleys were used (1 centered at the fetlock joint and 1 attached to the metacarpal segment at the level of the carpal joint). The proximal parts of the SDF and DDF tendons are not needed for the calculations. To quantify the parameters, 15 frozen right limbs were sectioned in the median plane. Origin and insertion of the tendons and position and radius of the pulleys were measured from photographs (2× magnification). Because the SL is not in the median plane at the level of the fetlock joint, an additional paramedian section was made through the insertion of the SL on the sesamoid bones. The radius of the fetlock pulley was measured directly from this section. Origin, insertion, and position of pulleys were expressed relative to a segment-based coordinate system. The origin of this coordinate system is the proximal joint, the x-axis runs through the distal joint, and the y-axis points cranially. For the hoof segment, the x-axis is parallel to the dorsal hoof wall. Values were standardized on the basis of segment length, and mean values were calculated over all limbs.

Evaluation of SDF tendon—To evaluate the SDF tendon, 8 left forelimbs were used. The proximal part of the SDF tendon was dissected free of surrounding tissue and transected at the muscle-tendon junction, but the insertion was allowed to remain intact. The metacarpus was transected immediately proximal to the fetlock joint (**Fig 2**). Infrared **light-emitting diodes (LED)** were used as markers for the strain measurements. Two LED on pins were inserted palmodorsally through the tendon at a mutual distance of approximately 14 cm. The pins were folded at the dorsal side of the tendon to secure the LED. Two additional markers were attached to the tendon markers for scaling purposes.[15]

The SDF tendons were tested in 2 conditions. They were initially loaded in a straight line and then loaded with a normal curvature around the fetlock joint. The proximal part of the tendon was clamped in a cryo-jaw[16] for both conditions. For straight loading, each hoof was affixed in a draw-bench, using a hoof clamp. After preconditioning loadings (10 times at 500 N), the tendon was loaded 3 times up to a force of 3 kN. For curved loading, each hoof was supported on a flat surface, and a bar was placed over the metacarpus (Fig 2). Angle of the fetlock joint was approximately 45°. After another series of preconditioning loadings, the tendon was loaded 3 times up to a force of 4 kN, and it then finally was loaded until failure. Strain rate was approximately 1.0 to 1.5%/s. During tendon loading, force was measured by use of a strain–gauge-based load cell[b] at a sample frequency of 100 Hz. Positions of the LED were measured by use of a 1-camera motion-analysis system[c] with a sample frequency of 60 Hz. The camera light was turned off to prevent reflections from the tendon. An additional LED, which was only active during acquisition of force data, was used for synchronization of the force and strain data.

Evaluation of SL—To evaluate the SL, 7 left forelimbs were used. Forelimbs were transected through the humerus immediately distal to the deltoid process. The SL was dissected free of surrounding tissue, and the metacarpal parts of the SDF and DDF tendons were removed. Two LED on pins were inserted palmodorsally through the SL at a mutual distance of approximately 10 cm. Similar to the evaluation of the SDF tendons, 2 additional LED were used for scaling. Four more LED were glued to the metacarpus and

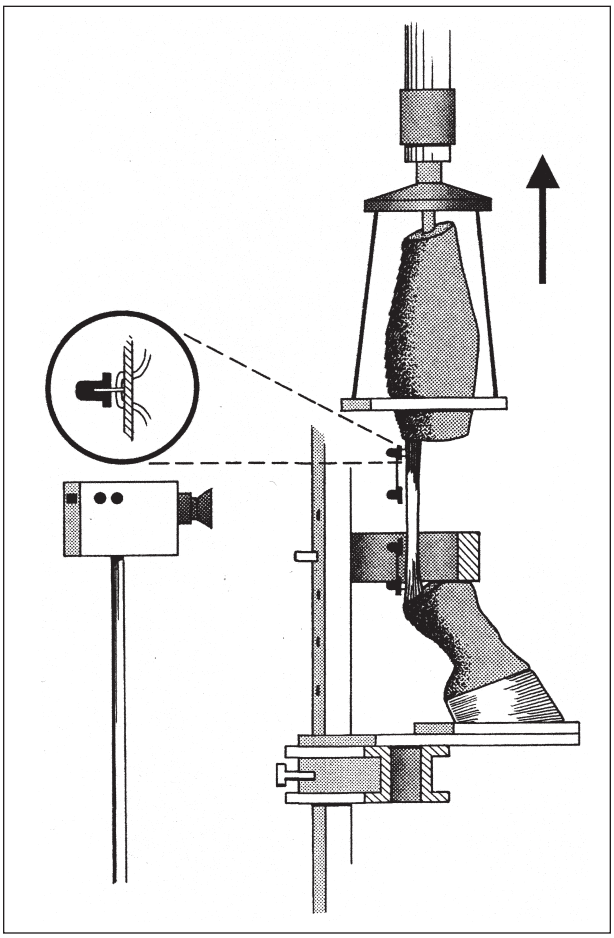

Figure 2—Illustration of the system used for curved loading of the SL. Loading of the SDF tendon was performed with a cryo-jaw instead of a carpal clamp. Force is exerted in the direction of the arrow.

the proximal phalanx to measure the angle of the fetlock joint.

Limb-loading experiments were performed to determine relationship between angle of the fetlock joint and ε_{SL}. Limbs were loaded on the humerus in a pneumatic-loading device to 2.5 kN (5 to 10 seconds) and unloaded to 0 kN. This was repeated 3 times. Positions of the tendon and bone markers during loading were measured, using the 1-camera motion-analysis system.[c] The camera had a direct palmar view of the tendon markers and an indirect lateral view of the bone markers via a mirror oriented at 45°. Reference measurements were made with additional markers on the carpal, fetlock, and coffin joints.

After the limb-loading experiments were completed, tendon-loading experiments were performed to determine the strain-force relationship. The radius was transected immediately proximal to the carpus, and the metacarpus was transected immediately distal to the carpus and also immediately proximal to the fetlock joint. Origin and insertion of the SL were allowed to remain intact. The carpus was attached to the draw-bench with a clamp (Fig 2). Apart from this, loading experiments for the SL were performed similar to loading experiments for the SDF tendon, except for slightly higher loads (10 preconditioning loadings at 1 kN, 3 straight loading measurements at 5 kN, 10 preconditioning loadings at 1 kN, 3 curved loading measurements at 5 kN, and loading until failure).

Evaluation of DDF tendon and AL—To evaluate the DDF tendon and AL, 5 right and 3 left forelimbs from 8 horses were used. Forelimbs were transected through the humerus, immediately distal to the deltoid process. The DDF tendon and AL were dissected free of surrounding tissue. The SDF tendon was removed, but the SL was allowed to remain intact. Pairs of LED were inserted mediolaterally through the AL, the proximal part of the DDF tendon (proximal to the insertion of the AL), and the distal part of the DDF tendon (distal to the fetlock joint). Intermarker distance for each pair of markers was approximately 4.5 cm. Pairs of LED were glued to the metacarpus, proximal part of the digit, and hoof to measure angles of the fetlock and coffin joints. The line through the pair of LED on the hoof was parallel to the dorsal hoof wall.

Limb-loading experiments were performed to determine the relationship between $L_{AL+DIST}$, ε_{DIST}, and ε_{AL}. To obtain various combinations of angles of the fetlock and coffin joints and to obtain various load distributions among the proximal part of the DDF tendon and AL, each limb was loaded in 3 positions (with the hoof flat, with the toe elevated, and with the heel elevated). Two repeated measurements were performed for each condition with loads up to 2.5 kN (hoof flat and heel elevated) or 2 kN (toe elevated). Reference measurements were made, using additional markers on the carpal, fetlock, and coffin joints. The 3-dimensional positions of the tendon and bone markers were measured, using a 2-camera motion-analysis system.[d] Scaling markers were not used. The system was calibrated before measurements, using dynamic calibration with the camera light turned on; the camera light was turned off during the measurements to prevent reflections.

After the limb-loading experiments, tendon-loading experiments were performed to measure the strain-force relationship of the 3 parts of the DDF tendon. The radius was transected immediately proximal to the carpus, and the limb was disarticulated at the fetlock and pastern joints. The proximal part of the DDF tendon was transected at the muscle-tendon junction. Tendon-loading experiments were performed in 2 stages. First, the AL and distal part of the DDF tendon were loaded. Second, the AL was transected, and the proximal and distal parts of the DDF tendon were loaded. Both systems were only loaded in a straight line to allow simultaneous visibility of all LED. For the AL-distal part of the DDF tendon measurements, the carpus and hoof were each affixed in position with a clamp. After preconditioning loadings (10 times to 500 N), the tendon was loaded 3 times up to 5 kN. For the measurement of the proximal and distal parts of the DDF tendon, the hoof was affixed in the clamp, and the proximal part of the tendon was clamped in a cryojaw. After another series of preconditioning loadings, (10 times to 500 N), the tendon was loaded once until failure. Strain was measured by use of the 2-camera motion-analysis system,[d] and force was measured by use of the load cell.[b] The systems were synchronized electronically and measured at a sample frequency of 30 Hz.

Data analysis for SDF tendon—The force data were resampled at a frequency of 60 Hz. Image deformations attributable to a nonperpendicular camera view were corrected by use of an oblique scaling algorithm.[15] Strain was calculated from the **distance between the markers (*L*)**, using the following equation, where the distance at a force of 100 N was used as **zero-length (L_0)**:

$$\varepsilon = \frac{L - L_0}{L_0}$$

The strain-force relationship was obtained by fitting a third-order polynomial through the force-versus-strain data. Only trials with a correlation coefficient between 0.99 and 1.00 were accepted. Strain at a force of 1, 2, and 3 kN was calculated from the strain-force relationships for the straight and curved tendon tests. Paired *t*-tests were used to test the influence of tendon curvature on these strains and L_0. Parameters of the strain-force relationship during final loading and the forces at failure were averaged over the 8 tendons.

Data analysis for SL—To account for a shift in L_0 between limb-loading and tendon-loading experiments,[17] L_0 was defined differently for both experiments. Distance between the markers when the limb was loaded only by its own weight was used as L_0 for the limb-loading experiments, whereas the distance at a force of 100 N was used for the tendon-loading experiments. Angle of the fetlock joint was calculated from the 2 lines through the bone markers. Reference measurements were used to correct the offset of this angle. Specific joint angle-strain relationships were obtained by fitting linear regression equations for the joint angle-strain data for each limb. The coefficients were averaged to obtain mean values for the 7 SL. Analysis of the tendon-loading experiments was similar to that described for the loading experiments of the SDF tendon.

Data analysis for DDF tendon and AL—For the limb-loading experiments, L_0 for each of the various parts of the tendon was defined as the distance between the respective marker pairs when the limb was loaded only by its own weight. The condition with the smallest distance was used. Joint angles were calculated from the bone markers, using the reference measurement for offset correction. The $L_{AL+DIST}$ was calculated from the joint angles, using the pulley model. For each limb, a multiple linear regression equation was fitted through the particular ε_{AL} versus $L_{AL+DIST}$ and ε_{DIST} data. Subsequently, the regression parameters were averaged to obtain 1 relationship between $L_{AL+DIST}$, ε_{DIST}, and ε_{AL}. For the tendon-loading experiments, length at a force of 100 N was used as L_0. Similar to the SL and SDF tendon experiments, third-order polynomials were fitted through the force-versus-strain data. For the AL, submaximal measurement with the largest peak force was used for each tendon. For the distal and proximal parts of the DDF tendon, final measurements were used. Parameters of the strain-

Table 1—Mean (SD) absolute and relative coordinates of the origin, insertion, and centers of the pulleys in a segment-based coordinate system (origin in the proximal joint, the x-axis running through the distal joint, and the y-axis pointing cranially) and radius of the pulleys

Tendon	Element	Segment	x (mm)	y (mm)	Radius (mm)	x (%)	y (%)
SDF	Pulley	Metacarpus	9.4 (6.8)	19.8 (6.3)	40.1 (6.1)	3.4 (2.4)*	7.2 (2.3)
	Pulley	Digit	0.0	0.0	52.5 (2.1)	0	0
	Insertion	Digit	108.3 (5.5)	–20.2 (1.3)	—	74.5 (1.1)*	–13.9 (0.9)
SL	Origin	Metacarpus	59.7 (5.7)	0.1 (4.7)	—	21.6 (2.1)	0.0 (1.7)
	Pulley	Digit	0.0	0.0	28.3 (1.8)	0.0	0.0
	Insertion	Digit	108.3 (5.5)	–20.2 (1.3)	—	74.5 (1.1)*	–13.9 (0.9)
DDF	Pulley	Metacarpus	9.4 (6.8)	19.8 (6.3)	40.1 (6.1)	3.4 (2.4)*	7.2 (2.3)
	Pulley	Digit	0.0	0.0	44.1 (2.4)	0.0	0.0
	Pulley	Hoof	3.9 (1.9)*	–10.3 (4.8)*	22.0 (3.9)	5.0 (2.7)	–13.1 (6.3)
	Insertion	Hoof	33.9 (1.9)*	–13.7 (2.2)*	—	42.5 (6.5)	–17.1 (3.1)
AL	Origin	Metacarpus	32.5 (8.2)	–6.8 (4.7)	—	11.7 (2.9)	–2.5 (1.7)

*When SD of absolute and relative coordinates differ by > 0.1% of the segment length, the smaller is indicated.
AL = Accessory ligament of the deep digital flexor tendon. DDF = Deep digital flexor tendon. SDF = Superficial digital flexor tendon. SL = Suspensory ligament. — = Not applicable.

force relationships and force at failure were averaged over the 8 tendons. To test the accuracy of the DDF tendon-AL model, $F_{DDFprox}$ during the limb-loading experiments was determined 2 ways (from the mean model and from the strain-force relationship of the proximal part of the DDF tendon). Root mean square of the difference between the 2 sets of forces was used to evaluate accuracy of the model.

Results

Pulley models—Mean and SD for parameters of the pulley models were determined (**Table 1**). In the hoof segment, the SD (expressed in percentage of segment length) of the variables was increased by standardization based on segment length, but in the other segments, the SD was reduced or not influenced by standardization.

SDF tendon—Third-order polynomials provided a good description of the strain-force data (**Fig 3**), and repeated measurements yielded similar results. We did not detect significant differences between the straight and curved loading: neither L_0 nor the strains at forces of 1, 2, or 3 kN differed significantly. Specific and mean strain-force relationships during the failure tests were determined (**Table 2**). Mean ± SD force at failure of 6 tendons was 11.9 ± 1.5 kN. All 6 failures were in the metacarpal part of the tendon. Force at failure for the remaining 2 tendons could not be determined because of inadequate fixation of the distal part of the limb.

SL—During the limb-loading experiments, angle of the fetlock joint increased from 16 ± 5° in unloaded limbs to 54 ± 4° in fully loaded limbs. Linear regression equations provided a good description of the angle of the fetlock joint-ε_{SL} relationships. Repeated measurements yielded similar results. The mean relationship is described by the following equation: ε_{SL} = –0.0234 + (0.00162 × angle of the fetlock joint [in degrees]).

During the tendon-loading experiments, there was a significant difference in L_0 between straight and curved loading experiments, but there was not a significant difference in strain values at forces of 1, 2, and 3 kN. Specific and mean strain-force relationships during the failure tests were determined (**Fig 4**). Parameters for the mean strain-force relationship were calculated (Table 2).

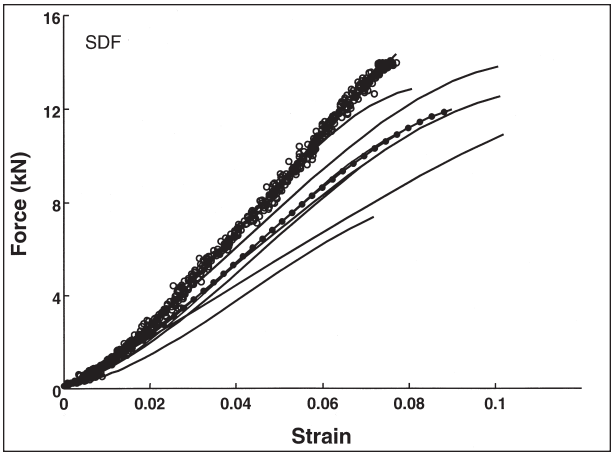

Figure 3—Strain-force relationship for the SDF tendon. Individual data points for 1 tendon (open circles), fitted relationships for each of 8 tendons (smooth lines), and the mean relationship for all tendons (line with solid circles) are plotted.

Table 2—Mean parameters for 6 to 8 tendons of the strain-force relationships of the flexor tendons in the equine forelimb and strain range for which they are valid

Tendon	Strain range	Parameters of the strain-force relationship			
		a_0	a_1	a_2	a_3
SDF	0.00–0.09	0.1	70.9	2.21×10^3	-1.70×10^4
SL	0.00–0.08	0.1	85.4	4.85×10^3	-4.29×10^4
DDF,dist	0.00–0.09	0.1	94.3	1.25×10^3	-5.32×10^3
DDF,prox	0.00–0.05	0.1	43.7	3.70×10^3	-3.65×10^4
AL	0.00–0.09	0.1	9.4	1.19×10^3	-7.47×10^3

DDF,dist = Distal part of the DDF tendon. DDF,prox = Proximal part of the DDF tendon.
For strain values within the indicated range, the force (in kN) can be calculated as follows: $F = a_0 + (a_1 \times \varepsilon) + (a_2 \times \varepsilon^2) + (a_3 \times \varepsilon^3)$.

Only 1 tendon was loaded until failure (14.6 kN). Ultimate forces for the other tendons were higher, but failure was not reached because of breakage of the carpal bones (2 tendons, 15 kN), limitation of the pulling force of the draw-bench (3 tendons, 15kN), or inadequate fixation of the distal part of the limb (1 tendon, 11 kN at a strain of 5%). To prevent excessive extrapolation of the data, we excluded data for the last tendon when calculating mean strain-force relationships.

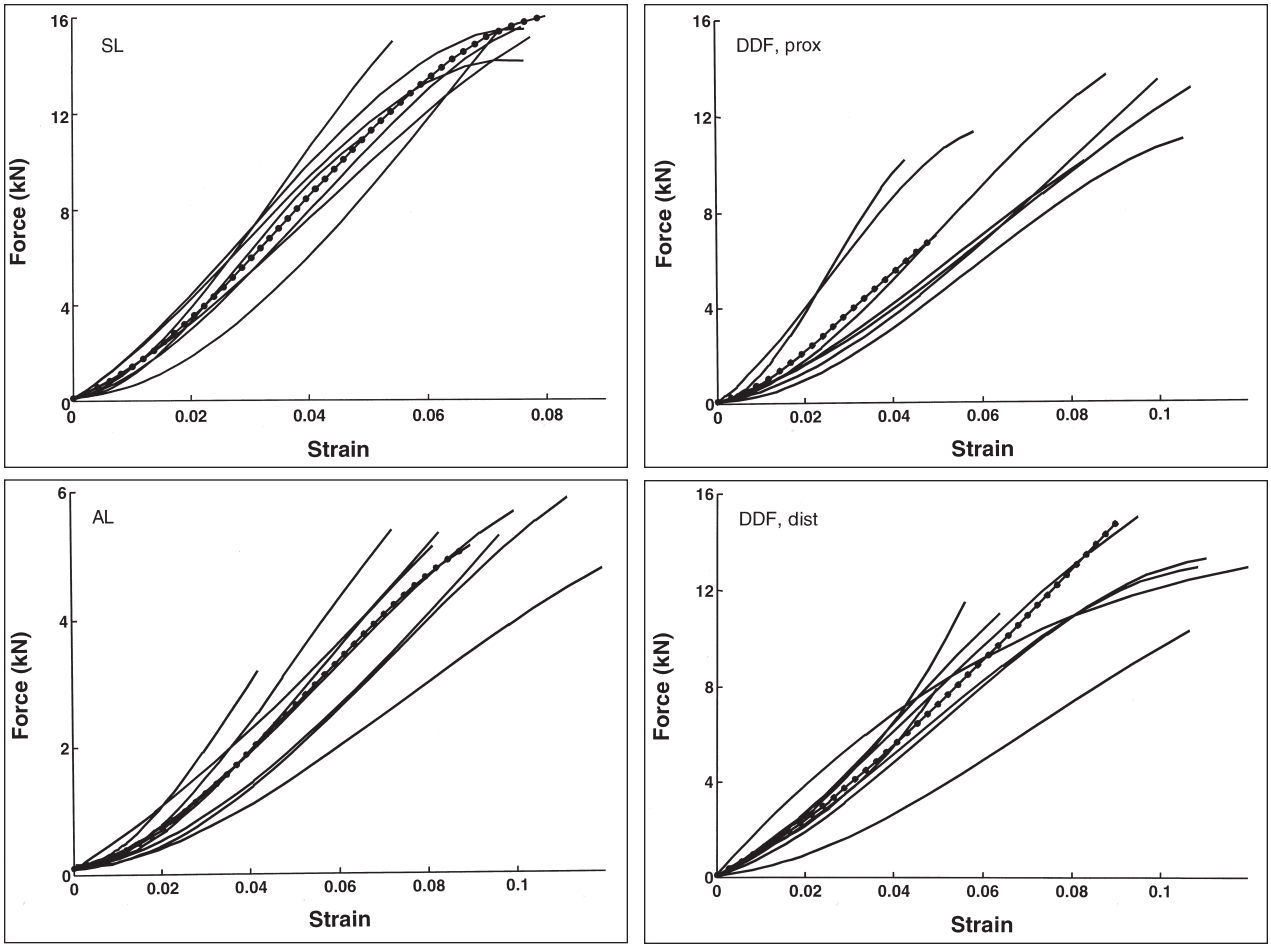

Figure 4—Strain-force relationship for the SL (upper left), proximal part of the DDF tendon (upper right), AL (lower left), and distal part of the DDF tendon (lower right). Each graph depicts fitted relationships for individual tendons (smooth lines) and the mean relationship for all tendons (line with closed circles). Notice that the scale for the x-axis differs for the SL, and the scale of the y-axis differs for the AL.

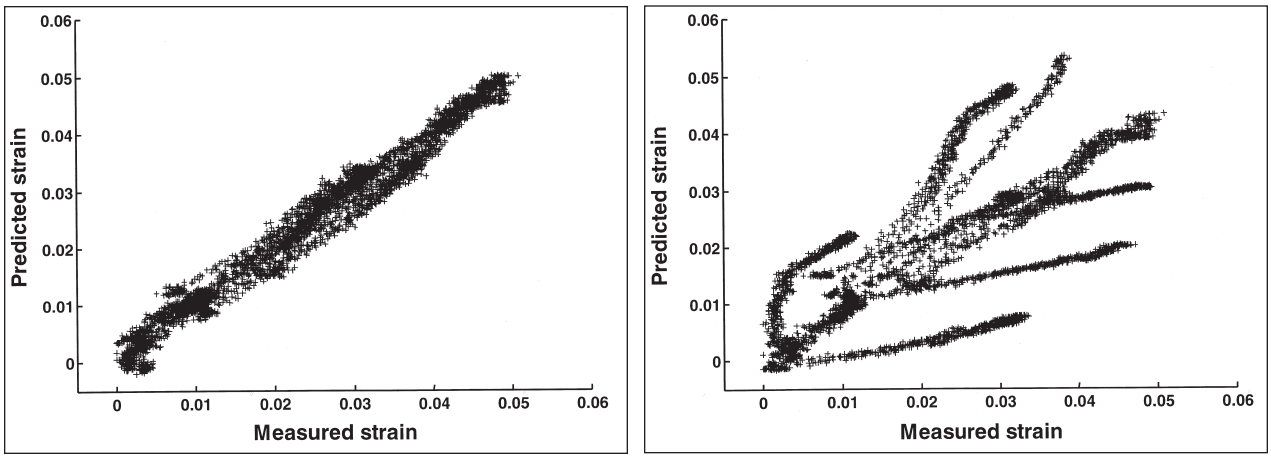

Figure 5—Prediction of strain for the AL as determined on the basis of individual regression equations (left) or the mean regression equation (right). All data points obtained during testing for 3 loading conditions of 5 limbs are indicated. Inputs for the regression equations are the origin-insertion length ($L_{AL+DIST}$) and strain in the distal part of the DDF tendon (ε_{DIST}).

DDF tendon and AL—The 3 loading conditions resulted in combinations of angles for the coffin and fetlock joints that clearly differed. Limb-loading data for 3 of the 8 limbs could not be used because of irregularities in the strain measurements or lack of strain in 1 or more parts of the tendon. Linear regression equations for each of the remaining 5 limbs had high regression coefficients (> 0.98; **Fig 5**). However, the interindividual variability in regression parameters was high, and estimation of ε_{AL} from the mean regression equation resulted in large errors. For most limbs, ε_{AL} was mainly determined by $L_{AL+DIST}$, and the contribu-

tion of ε_{DIST} to the explained variance was small (typical increase in squared regression coefficient, 5%).

Interindividual variability of the force-strain relationships of the AL and distal and proximal parts of the DDF tendon was larger than variability of the SL relationships (Fig 4). Mean parameters of the strain-force relationships of the AL and distal and proximal parts of the DDF tendon were calculated (Table 2). Mean force at failure of 6 tendons was 13.0 ± 1.5 kN. Five tendons ruptured proximal to the insertion of the AL, and 1 tendon ruptured distal to the AL insertion. Force at failure for the remaining 2 tendons could not be determined because of inadequate tendon fixation or errors in data acquisition. To prevent excessive extrapolation of the data, only a limited part of the strain-force relationships of the proximal part of the DDF tendon was calculated.

Because of the large interindividual variation, application of the mean model on the data for each tendon resulted in large differences between $F_{DDFprox}$ calculated from the model and force calculated from the strain-force relationship of the proximal part of the DDF tendon (absolute and relative root mean square error > 3 kN and >100%, respectively).

Discussion

The study reported here described a method to calculate flexor tendon forces on the basis of on an in vitro model and quantified parameters of that model.

The pulley model has been applied successfully in ponies[18,19] and should be equally applicable in horses. The only major difference with the previously described model can be found at the level of the carpal joint. In the previous model, the pulleys were on the caudal side of the SDF and DDF tendons, whereas in the model reported here, they were on the cranial side. A caudal location of the pulleys provides a better description of the line of action during flexion of the carpus, whereas a cranial location of the pulleys provides a better description during hyperextension. Because the model described here will be used during the stance phase, hyperextension is more likely than flexion. Therefore, pulleys located on the cranial aspect are the better choice. Apart from this, the standardized values are similar to those determined in ponies. The radii of the pulleys are approximately 25 to 30% larger in horses, which is reasonable, because they have segments that are 20 to 30% longer. Insertions of the SL and SDF tendon are nearly the same for both models, whereas the origins of AL and SL are more proximal and slightly more cranial in the horses. However, this may only be a reflection of a difference in definition of the tendon-bone transition on the same line of action. Values for the distal part of the DDF tendon were smaller in the ponies but could not be standardized, because the hoof length of the ponies was unknown.

To account for interindividual differences in size, values were standardized to segment length. For most variables, this reduced the variability. However, variability increased for the hoof segment. Hoof length depends primarily on growth and wear and does not reflect the constant internal dimensions of the segment. In the application of the model, best results will be obtained when absolute data are used for the hoof segment and standardized data for the other segments.

In tendon-loading experiments in other studies,[1,20,21] tendons were mostly loaded in a straight line. However, during normal function, the SDF tendon is curved around the fetlock joint. To provide a more physiologic loading of the tendon, the study we conducted was performed with the tendon curved around the fetlock joint. In addition, we tested whether curvature influenced the results. Differences were not found in submaximal strain-force relationships. However, results may have differed if strain also had been measured in the curved part of the tendon. Furthermore, the influence of curvature on force of failure was not determined. Because the straight metacarpal portion is the weakest part of the SDF tendon in vivo and in vitro, it is unlikely that the force of failure was influenced by curvature of the more distal part of the tendon. Therefore, it seems justified to use either straight or curved loading when determining the mechanical properties of the metacarpal part of the flexor tendons.

The inflection point, the strain at which the slope of the strain-force curve reaches its maximum, has been used as a measure of strength of tendons.[20] However, in the study reported here, a consistent inflection point could not be determined. Although the strain-force relationships of the repeated submaximal measurements resembled each other, there were large differences in inflection point. This was probably caused by the fact that the inflection point is determined from the second derivative of the strain-force curve, which is sensitive to small changes in the data. Instead of the inflection point, force of failure was used as a measure of strength of the tendons. Forces at which the SDF tendons failed in this study agree well with those reported elsewhere.[20,e]

Calculation of SL strain on the basis of the angle of the fetlock joint has been validated in ponies and smaller horses[5] and should be equally valid for larger horses. Our results are quite similar to those reported previously, which could be expected because of similarities in parameters of the pulley model.

Limb-loading experiments were combined with tendon-loading experiments. It is known that there are shifts in L_0 between differing loading conditions.[17] In the experiments conducted here, use of the same L_0 for both experiments would have resulted in large and unrealistic variations in angles of the fetlock joint at L_0 for the SL (eg, substantial flexion instead of extension). Furthermore, there was a shift in L_0 between straight and curved loading. Therefore, different definitions of L_0 were used for both loading experiments, although final results might be sensitive to the definition of L_0. Defining L_0 at a force of 50 or 200 N instead of 100 N resulted in minor errors in calculated force (< 0.4 kN), but shifting the angle of the fetlock joint used to determine L_0 by 5° resulted in errors of up to 2 kN.

Unfortunately, it was not possible to determine the ultimate strength of the SL. It is possible that other clamping techniques must be used. It is tempting to clamp the proximal part of the SL in a cryo-jaw. However, this might yield invalid results, because the insertion is not included in the test. Although the SL

was not ruptured, the results reported here indicate that the SL is the strongest flexor in the forelimb of adult horses. This is in agreement with results obtained in ponies.[f]

DDF tendon and AL—The available distance for marker placement in the DDF tendon and AL is much smaller than in the SDF tendon and SL. This limits the possibility of attaching additional scaling markers. To minimize the number of markers, strain was measured by use of a 2-camera motion-analysis system with only 2 markers in each part of the tendon.

For several reasons, accuracy of measurements for the DDF tendon and AL was less than accuracy of measurements for the other tendons. First, boundaries of the AL are less clearly defined than boundaries of the other tendons. Differences in dissection between the ligaments may have added to interindividual variability. Second, the markers were inserted mediolaterally to enable simultaneous measurement of AL and the distal part of the DDF tendonIt is more difficult to secure the markers by folding the pins at the lateral side than at the dorsal side. Furthermore, longer pins are needed, which might cause damage to the tendon. Finally, because of the smaller distance between the markers, noise and measurement errors have a larger influence on accuracy of strain measurements. Because of this, the strain-force relationships of the DDF tendon and AL are only an approximation.

The smaller accuracy and large interindividual variability caused large deviations between $F_{DDFprox}$ calculated from the model and $F_{DDFprox}$ calculated from the strain-force relationship for the proximal part of the DDF tendon. Although the definition of L_0 influences the calculated forces, the use of other definitions of L_0 did not improve the results. On the basis of the results reported here, it was not possible to accurately determine F_{AL} and $F_{DDFprox}$ from noninvasive measurements. However, the individual regression equations for AL strain had high regression coefficients. Furthermore, they were barely influenced by strain in the distal part of the tendon. This is probably caused by a higher stiffness of the distal part of the tendon. Because of this, $L_{AL+DIST}$ can be used as a measure of AL loading for within-subject comparisons. For example, it can be used to verify whether muscle fatigue causes additional loading of the AL.

The study reported here described a noninvasive method to calculate flexor tendon forces in the equine forelimb. The method is based on inverse dynamic calculation of joint moments. Contrary to most other inverse dynamics-based models, it does not use optimizations or EMG data to distribute joint moments among the available muscles. Instead, it uses the mechanical properties of the passive structures to solve the indeterminacy of the system. This solution is only valid if there are not any extensor forces. On the basis of results of EMG[22] and simulation[a] studies, it can be assumed that extensor forces are negligible during the stance phase of walking and trotting. However, during other activities, there may be substantial extensor forces that limit the applicability of this method.

Furthermore, the validity of this method should be tested before the method is applied. The calculations are based on extrapolation of an in vitro model to live horses. Because there is interindividual variability in tendon properties (Fig 3 and 4), differences between the properties of individual tendons of a horse used for the in vivo measurements and the mean in vitro model might introduce errors in the calculations. Furthermore, accuracy of the in vivo measurements of ground-reaction forces and kinematics is limited. Errors in these measurements also could introduce errors in the calculations. Before application of the model, it is important to determine the influence of those model and measurement errors on the calculated forces.[23]

The model described in the study reported here enables noninvasive determination of forces in the SL, SDF tendon, and distal part of the DDF tendon. In addition, it provides a noninvasive measure of loading of the AL for within-subject comparisons. It can become an important tool for use in research of the cause, prevention, and treatment of tendon injuries in horses. However, before application, the method should be validated.

[a]van den Bogert AJ. *Computer simulation of locomotion in the horse.* PhD thesis, University of Utrecht, Utrecht, the Netherlands, 1989.
[b] Sangamo TCLP-2B, Sokki Kenkyujo & Co Ltd, Tokyo, Japan.
[c]Mac-Reflex, Qualisys, Sävedalen, Sweden,
[d]Pro-Reflex, Qualisys, Sävedalen, Sweden,
[e]Wilson AM, Goodship AE. Mechanical properties of the equine superficial digital flexor tendon (SDFT) (abstr). *J Biomech* 1994; 24:474.
[f]Jansen MO. *Tendon strain, force and function in equine locomotion.* PhD thesis, University of Utrecht, Utrecht, the Netherlands, 1995.

References

1. Lochner FK, Milne DW, Mills EJ, et al. In vivo and in vitro measurement of tendon strain in the horse. *Am J Vet Res* 1980;41:1929–1937.
2. Jansen MO, van den Bogert AJ, Riemersma DJ, et al. In vivo tendon forces in the forelimb of ponies at the walk, validated by ground reaction force measurements. *Acta Anat (Basel)* 1993;146:162–167.
3. Platt D, Wilson AM, Timbs A, et al. Novel force transducer for the measurement of tendon force *in vivo*. *J Biomech* 1994;27: 1489–1493.
4. Bartel DL, Schryver HF, Lowe JE, et al. Locomotion in the horse: a procedure for computing the internal forces in the digit. *Am J Vet Res* 1978;39:1721–1727.
5. Jansen MO, van Buiten A, van den Bogert AJ, et al. Strain of the musculus interosseus medius and its rami extensorii in the horse, deduced from in vivo kinematics. *Acta Anat (Basel)* 1993;147: 118–124.
6. van den Belt AJ, Dik KJ, Barneveld A. Ultrasonographic evaluation and long-term follow-up of flexor tendonitis/desmitis in the metacarpal/metatarsal region in Dutch warmblood horses and standardbred racehorses. *Vet Q* 1994;16(suppl 2):S76–S80.
7. Crowninshield RD, Brand RA. A physiologically based criterion of muscle force prediction in locomotion. *J Biomech* 1981; 14:793–801.
8. Paul JP. Load actions on the human femur in walking and some resultant stresses. *Exp Mech* 1971;11:121–125.
9. Cholewicki J, McGill SM, Norman RW. Comparison of muscle forces and joint load from an optimization and EMG assisted lumbar spine model: towards development of a hybrid approach. *J Biomech* 1995;28:321–331.
10. Prilutsky BI, Herzog W, Allinger TL. Forces of individual cat ankle extensor muscles during locomotion predicted using static optimization. *J Biomech* 1997;30:1025–1033.
11. Herzog W, Leonard TR. Validation of optimization models that estimate the forces exerted by synergistic muscles. *J Biomech* 1991;24:31–39.

12. Meershoek LS, Schamhardt HC. A non-invasive method to determine in vivo forces of equine digital tendons, in *Proceedings*. 11th Int Biomech Semin 1998;87–92.

13. Elftman H. Forces and energy changes in the leg during walking. *Am J Physiol* 1939;125:339–356.

14. Meershoek LS, van den Bogert AJ. Mechanical analysis of locomotion. In: Back W, Clayton H, eds. *Equine locomotion*. London: WB Saunders Co, 2000;305–326.

15. Meershoek LS, Schamhardt HC. Oblique scaling: an algorithm to correct for a non-perpendicular camera view in tendon strain measurements. *J Biomech* 2000;33:1529–1532.

16. Riemersma DJ, Schamhardt HC. The cryo-jaw, a clamp designed for in vitro rheology studies of horse digital flexor tendons. *J Biomech* 1982;15:619–620.

17. Riemersma DJ, Lammertink JL. Calibration of the mercury-in-silastic strain gauge in tendon load experiments. *J Biomech* 1988; 21:469–476.

18. van den Bogert AJ, Schamhardt HC. Multi-body modelling and simulation of animal locomotion. *Acta Anat (Basel)* 1993;146:95–102.

19. Riemersma DJ, van den Bogert AJ, Schamhardt HC, et al. Kinetics and kinematics of the equine hind limb: in vivo tendon strain and joint kinematics. *Am J Vet Res* 1988;49:1353–1359.

20. Crevier N, Pourcelot P, Denoix JM, et al. Segmental variations of in vitro mechanical properties in equine superficial digital flexor tendons. *Am J Vet Res* 1996;57:1111–1117.

21. Jansen MO, Savelberg HHCM. Stress and strain of equine tendons of the forelimb at failure. *Equine Vet J* 1994;17(suppl):57–60.

22. Jansen MO, van Raaij JA, van den Bogert AJ, et al. Quantitative analysis of computer-averaged electromyographic profiles of intrinsic limb muscles in ponies at the walk. *Am J Vet Res* 1992;53:2343–2349.

23. Meershoek LS, Lanovaz JL. Sensitivity analysis and application to trotting of a noninvasive method to calculate flexor tendon forces in the equine forelimb. *Am J Vet Res* 2001;62:1594–1598.